Geometries, stabilities, and electronic properties analysis in $In_nNi^{(0,\pm1)}$ clusters: Molecular modeling and DFT calculations*

Shun-Ping Shi(史顺平)[1], Chuan-Yu Zhang(张传瑜)[1,†], Xiao-Feng Zhao(赵晓凤)[1], Xia Li(李侠)[1], Min Yan(闫珉)[1], and Gang Jiang(蒋刚)[2]

[1] *Department of Applied Physics, College of Geophysics, Chengdu University of Technology, Chengdu* 610059, *China*
[2] *Institute of Atomic and Molecular Physics, Sichuan University, Chengdu* 610065, *China*

(Received 23 March 2017; revised manuscript received 4 May 2017; published online 10 July 2017)

Density functional theory (DFT) with the B3LYP method and the SDD basis set is selected to investigate In_nNi, In_nNi^-, and In_nNi^+ (n = 1–14) clusters. For neutral and charged systems, several isomers and different multiplicities are studied with the aim to confirm the most stable structures. The structural evolution of neutral, cationic, and anionic In_nNi clusters, which favors the three-dimensional structures for n = 3–14. The main configurations of the In_nNi isomers are not affected by adding or removing an electron, the order of their stabilities is also nearly not affected. The obtained binding energy exhibits that the Ni-doped In_{13} cluster is the most stable species of all different sized clusters. The calculated fragmentation energy and the second-order energy difference as a function of the cluster size exhibit a pronounced even–odd alternation phenomenon. The electronic properties including energy gap (E_g), adiabatic electron affinity (AEA), vertical electron detachment energy (VDE), adiabatic ionization potential energy (AIP), and vertical ionization potential energy (VIP) are studied. The total magnetic moments show that the different magnetic moments depend on the number of the In atoms for charged In_nNi. Additionally, the natural population analysis of $In_nNi^{(0,\pm1)}$ clusters is also discussed.

Keywords: $In_nNi^{(0,\pm1)}$ clusters, stability, electronic property, density functional theory

PACS: 31.15.E–, 36.40.Mr, 36.40.Cg **DOI:** 10.1088/1674-1056/26/8/083103

1. Introduction

Atomic clusters play a bridge between molecular and condensed matter physics. Therefore, the properties of clusters are widely studied as a function of size and composition with two objectives: First, researcher hopes to learn how they evolve toward bulk properties and to find unique properties for specific cluster sizes that differ largely from their bulk counterparts. Second, when the composition varies, corresponding to the structure, stability, electronic property, magnetic moment, etc. are also changed. These characteristics make a huge potential of clusters studies for a wide range of applications. In recent years, semiconductor nanomaterials have drawn a lot of research efforts both for theoretical and for their potential technological applications. Indium as a good semiconductor element, the technological importance is growing due to its potential mainstream use in future nanoelectronic devices.[1] Thus, over the past decades, the structural and electronic properties of indium clusters have been extensively studied both experimentally and theoretically.[2–11] For example, Staudt and Wucher[11] investigated the yields of neutral and charged In_n clusters sputtered from a pure indium surface under bombardment with 15-keV Xe^+ ions, the results demonstrated that for clusters containing more than about 20 atoms the detection probability became an exceedingly important parameter that needed to be characterized in order to arrive at a quantitative determination of the true cluster size distribution.

However, a great number of experimental and theoretical works about doped indium clusters have been studied.[12–31] This is motivated by the fact that an atom doped in a small indium cluster can strongly change the properties of the pure indium cluster. Janssens *et al.*[12] performed the structures and ionization potentials of small In_nO clusters (n = 1–8) by using experimental and theoretical studies, they found that ionization potentials were slightly lower for the In_nO species than for pure indium clusters and exceptionally low ionization potentials were obtained for In_3O and In_7O. When one N atom is doped In_n clusters, the In_3N, In_7N, and In_9N clusters possesses relatively higher stability than their neighbor.[13] However, when two N atoms are doped In_n clusters, In_8N_2 cluster is the strongest of all the investigated clusters.[16] In addition, the calculated results of In_xP_x and $In_xP_x^-$ clusters showed that hollow cages with alternating In–P bonds were energetically preferred over other structures for both the neutral and anionic species within the range x = 6–15.[14] Except the metalloid element is doped, the metal element and the transition metal

*Project supported by the Cultivating Program of Excellent Innovation Team of Chengdu University of Technology (Grant No. KYTD201704), the Cultivating Program of Middle-aged Backbone Teachers of Chengdu University of Technology (Grant No. 10912-KYGG201512), the National Natural Science Foundation of China (Grant No. 11404042), the Science Fund from the Science & Technology Department of Sichuan Province, China (Grant No. 2016RZ0069), and the Research Foundation of Chengdu University of Technology, China (Grant No. 2017YG04).

†Corresponding author. E-mail: zhangchuanyu10@cdut.cn

© 2017 Chinese Physical Society and IOP Publishing Ltd

(TM) element are also doped,[15,17–21,23,24,27,28] because the metal element and TM element alter just one atom's presence, location, or identity. Based on the above facts, Liu *et al.*[20] investigated the stabilities and electronic properties of In_nNa_2 ($n = 4$–9) clusters, in comparison with the corresponding pure In_n clusters, the doped Na atoms resulted on a local structural distortion of the mixed clusters. Both the $PbIn_3^-$ and Pb_2In_2 clusters,[19] which had planar, C_{2v} ground state geometries, large HOMO–LUMO (highest occupied molecular orbited–lowest unoccupied molecular orbital) gaps of 1.34 eV and 1.45 eV, respectively. By anionic photoelectron spectroscopy and fist principles calculations, Gupat *et al.*[27] obtained that the Bi_2In^-, $Bi_3In_2^-$, Bi_4In^-, and Bi_4In_2 were classified as gas phase zintl clusters that followed Wade's rules and were analogous to known zintl species.

All the time, TM element-doped clusters have attracted attention, because when a transition metal is encapsulated into clusters, some special phenomena appear, for example, when the Ti atom is doped to Ga_n clusters, the average binding energies exhibit a sequence as $Ga_nTi^- > Ga_nTi^+ > Ga_nTi > Ga_{n+1}$, and the HOMO–LUMO gaps of Ga_nTi clusters are distinctly higher than those of Ga_{n+1} clusters.[32] When the Nb atom is doped Ga_n clusters, the results indicated the doping of Nb atom in gallium clusters improved the chemical activities.[33] Ni atom as a TM element, it is usually selected to dope the clusters.[34–40] For instance, the averaged binding energies of the $NiGe_n$ clusters were obviously higher than those of the pure Ge_n clusters, which indicated that the doped Ni atom in the Ge_n clusters contributes to strengthen the stabilities of the germanium framework.[34] Yuan *et al.*[36] found that the odd–even alterations of vertical detachment energies were shown markedly in Ni-doped gold clusters, therefore, they predicted that the odd–even alteration of the reactivity of O_2 can be found on Ni-doped gold clusters. In this paper, to compare the effect of the doped Ni atom to the indium clusters, using the first-principles method based on density-functional theory, we systematically investigate the indium clusters-doped Ni atom, $In_nNi^{(0,\pm1)}$ ($n = 1$–14). In the case of doping with nickel, Ni atom delivers just also one itinerant electron because of the small promotion energy from $3d^84s^2$ to $3d^94s^1$ with respect to other 3d transition elements.[39] Therefore, these systems have a contribution in clarifying the influence of the s-, d-electrons of impurity atoms on geometric, electronic, and bonding properties of dopant indium clusters with respect to pure indium clusters.

2. Computational details

A research is performed for the lowest energy and low-lying structures of $In_nNi^{(0,\pm1)}$ ($n = 1$–14) clusters, using the density functional theory (DFT). In this paper, we employ a combination functional of Becke's three-parameter exchange functional (B3)[41] with the Lee–Yang–Parr (LYP)[42] generalized gradient correction functional. In addition, in order to confirm the structures and energies of all neutral, anionic, and cationic $In_nNi^{(0,\pm1)}$ clusters, the basis set SDD[43] is chosen, in which the core electrons is constituted by energy-consistent 21-valence electron relativistic effective core potential (RECP) of the Stuttgart group. The other functionals (B3P86, B3PW91) and other basis sets (LanL2DZ, DZVP) on the two-atom clusters (In_2 and Ni_2) are checked, with the purpose to choose the suitable computational method. The calculated results together with the comparable experimental and theoretical results are listed in Table 1. From Table 1, we see that the values of functionals (B3P86, B3PW91) and basis sets (LanL2DZ, DZVP) do not depend on that experimental results, however, it can be found that the experimental results for bond length (R_e), vibration frequencies (ω_e), dissociation energies (D_e), and ionization potentials (IP) are quite matched to the choices of B3LYP method and SDD basis set.

Table 1. Calculated values of bond length R_e (in unit Å), frequency ω_e (in unit cm^{-1}), dissociation energy D_e (in unit eV), and ionization potentials IP (in unit eV) for the In_2 and Ni_2 molecules at different levels.

Molecule	Method		R_e/Å	ω_e/cm^{-1}	D_e/eV	IP/eV
In_2	B3LYP	LanL2DZ	3.190	98.6	1.03	5.37
		SDD	2.871	123.3	0.83	5.81
	B3P86	LanL2DZ	3.159	104.1	1.18	6.03
		SDD	2.835	133.7	1.03	6.50
	B3PW91	LanL2DZ	3.164	104.0	1.16	5.54
		SDD	2.837	134.1	1.01	6.01
	Theory		3.084[a]	110.2[a]	1.05[a]	–
	Experiment		2.83[b]	118.0[c]	0.972[d] 1.002[e]	5.8±0.3[d]
Ni_2	B3LYP	LanL2DZ	2.377	232.3	1.59	7.14
		SDD	2.375	228.3	1.52	6.97
	B3P86	LanL2DZ	2.352	242.5	1.69	7.67
		SDD	2.349	238.2	1.53	7.50
	B3PW91	LanL2DZ	2.369	236.0	1.55	7.06
		SDD	2.363	233.3	1.41	6.89
	Theory		2.11[f]	325[f]	2.50[f]	7.86[f]
	Experiment		2.20[g]	259.2[h]	2.068[g]	7.43[i]

[a]Ref. [7], [b]Ref. [45], [c]Ref. [8], [d]Ref. [21], [e]Ref. [46], [f]Ref. [47], [g]Ref. [48], [h]Ref. [49], [i]Ref. [50].

For small-sized neutral, cationic, and anionic $In_nNi^{(0,\pm1)}$ ($n = 1$–14) clusters, a great deal of isomers are considered, including all the configurations in the literature. Then, both some independent configurations and we optimized several isomeric structures by placing an Ni atom on each possible site of the In_n cluster or by adding one In atom to the $In_{n-1}Ni$ cluster as well as by substituting one In by Ni atom form the In_{n+1} cluster, we obtain the lowest energy structures of In_nNi clusters. We also implement configurations calculations to gain ground state structures of $In_nNi^{\pm1}$ ($n = 1$–14) clusters. For $In_nNi^{\pm1}$ ($n = 1$–14) clusters, we consider that the structures of In_nNi clusters will be directly developed into the structures of $In_nNi^{\pm1}$ clusters. In addition, the default self-consistent field convergence to 10^{-8} a.u. (The unit a.u. is short for atomic unit) and (75, 302) integral pruned grid are used, which are exactly enough to ensure that the results are valid. For each configuration, three different spin multiplicities for $In_nNi^{(0,\pm1)}$ clusters are considered. The structures with the lowest energies are chosen as the ground-state configurations. All calculations are performed using the Gaussian 03W package.[44]

3. Results and discussion

3.1. Geometrical structures of $In_nNi^{(0,\pm1)}$ ($n \equiv 1$–14) clusters

For $In_nNi^{(0,\pm1)}$ ($n = 1$–14) clusters, a lot of initial possible geometries with various possible spin multiplicities are optimized. The optimized most stable and low-lying structures of In_nNi, In_nNi^{-1}, and In_nNi^{+1} clusters are plotted in Fig. 1, Fig. 2, and Fig. 3, respectively. According to the relative energy from low to high, the stability orders of each cluster are marked by order of letter, $na > nb > nc >$ and so on (n is the number of In atoms in $In_nNi^{(0,\pm1)}$ clusters), meanwhile, the symmetries of In_nNi, In_nNi^{-1}, and In_nNi^{+1} clusters are also listed in Fig. 1, Fig. 2, and Fig. 3, respectively.

(i) InNi, $InNi^-$, and $InNi^+$

The equilibrium geometries of $InNi^{(0,\pm1)}$ clusters with $C_{\infty v}$ symmetry are optimized. The doublet InNi dimmer is the ground state, and the corresponding electronic state is $^2\Sigma$, the bond length of InNi dimmer is 2.656 Å. However, the bond lengths of triplet $InNi^-$ and triplet $InNi^+$ dimmer are 2.597 Å and 2.657 Å, which are shorter and longer than the bond length of neutral InNi, reflecting that the In–Ni interaction of the neutral InNi is weaker than the In–Ni interaction of the anionic $InNi^-$ and stronger than the In–Ni interaction of the cationic $InNi^+$, respectively.

(ii) In_2Ni, In_2Ni^-, and In_2Ni^+

The possible structures such as C_{2v}, $C_{\infty v}$, and $D_{\infty v}$ isomers are optimized as the stable structures. According to the optimized results, it is worth noting that the lowest-energy structures as shown in Fig. 1 (2a), Fig. 2 ($2a^-$), and Fig. 3 ($2a^+$) are an isosceles triangle in which the bond lengths are 2.63 Å, 2.68 Å, 2.74 Å for In–Ni, respectively. We obtain the bond angles are 69.8°, 68.3°, 129.8° for In–Ni–In, respectively. Although the isomer $2a^-$ is similar to the lowest-energy structure of the 2a, the isomer $2a^+$ is different to the lowest-energy structure of the 2a. The linear structures 2b and $2b^-$ with Ni atom at one end are the next isomer, but the linear structure $2b^+$ with Ni atom in the middle is the next isomer.

(iii) In_3Ni, In_3Ni^-, and In_3Ni^+

In the case of $n = 3$, In_3Ni, In_3Ni^-, and In_3Ni^+ have the same most stable structure (3a, $3a^-$, and $3a^+$ in Fig. 1, Fig. 2, and Fig. 3, respectively), which are a three-dimensional tetrahedral configurations, the symmetries are C_{3V}. The other two geometries for the neutral In_3Ni clusters are a planar quadrilateral structure and a planar Y-shaped structure, whose relative energies are 0.308 eV, 0.873 eV and the symmetries are C_{2V}, and C_S, respectively. Correspondingly the orders of relative energies of anionic and cationic In_3Ni clusters are same with neutral In_3Ni clusters, in which the symmetries are also C_{2V}, and C_S, respectively.

(iv) In_4Ni, In_4Ni^-, and In_4Ni^+

For $n = 4$, the lowest-energy structures of the neutral, cationic, and anionic In_4Ni clusters are same, and the symmetries C_{4V} of all of them are also identical. The ground-state structure of the In_4Ni cluster with the electron state $^3B_1$ is different from the ground state structure of the In_5 cluster.[51] The 4b and 4c isomers with C_{2V} and C_{3V} symmetries are higher in energy than the most stable structure 4a by 0.64 eV and 0.88 eV, respectively. The energy orders of anionic $4b^-$ with C_{2V}, $4c^-$ with C_{3V}, and cationic $4b^+$ with C_{2V}, $4c^+$ with C_{3V} are same with neutral 4b and 4c.

(v) In_5Ni, In_5Ni^-, and In_5Ni^+

Starting $n = 5$, the lowest energy structures for neutral and cationic forms are similar, but the most stable structure of anionic cluster is different with neutral and cationic forms, although the symmetries of In_5Ni, In_5Ni^-, and In_5Ni^+ clusters are identical (C_S). The structures and the energy orders of 5b, 5c and $5b^-$, $5c^-$ with C_{4V} and C_{5V} symmetries are also similar. Although the structures of $5b^+$ and $5c^+$ are same with 5c and 5b, respectively, the energy orders are also contrary.

(vi) In_6Ni, In_6Ni^-, and In_6Ni^+

By calculations, we obtain that the spin triplet state is the lowest energy for the In_6Ni cluster (Fig. 1 (6a)), corresponding to the $^3A''$ state and the C_S symmetry. The most stable structures of In_6Ni^- and In_6Ni^+ are also prism structures, which are in agreement with the neutral In_6Ni cluster. The difference is that the energy orders for the isomers of cationic are different with the neutral and the anionic.

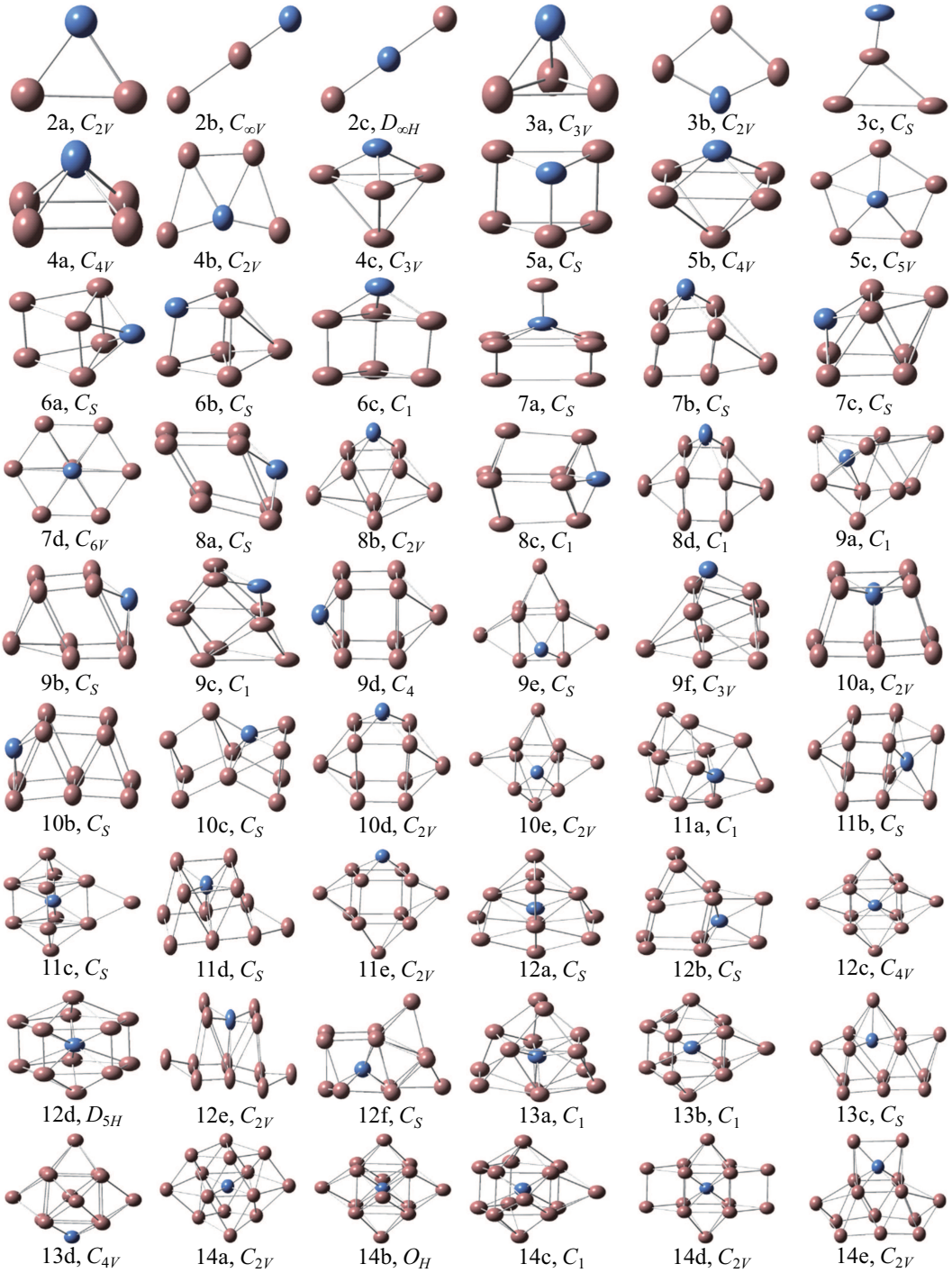


Fig. 1. (color online) The lowest energy and low lying structures of In_nNi ($n = 1$–14) clusters.

(vii) In_7Ni, In_7Ni^-, and In_7Ni^+

The global minimum of In_7Ni cluster can be generated by adding an In atom to the corresponding In_6Ni cluster. The most stable structures for the cationic and the anionic clusters are similar to those of its neutral counterparts, and the symmetries are also identical, which are C_S. The only difference is that the neutral with the $^2A'$ state instead of $^1A'$ state of the cationic and the anionic. Also, the other stable isomers for the three clusters, the orders of stabilities are different ($7b^-$, $7c^-$, and $7b^+$, $7c^+$ are same, 7b, 7c, and $7b^-$, $7c^-$ are different).

(viii) In_8Ni, In_8Ni^-, and In_8Ni^+

In the case of the most stable In_8Ni, we optimize the geometry subject to capped octahedron geometry with C_S symmetry. The structure is in reasonable agreement with the anionic but different to the cationic, this structure is the third most stable for In_8Ni^-, and the most stable structure of In_8Ni^- favors that Ni atom is located in the inside of the distorted capped trigonal prism.

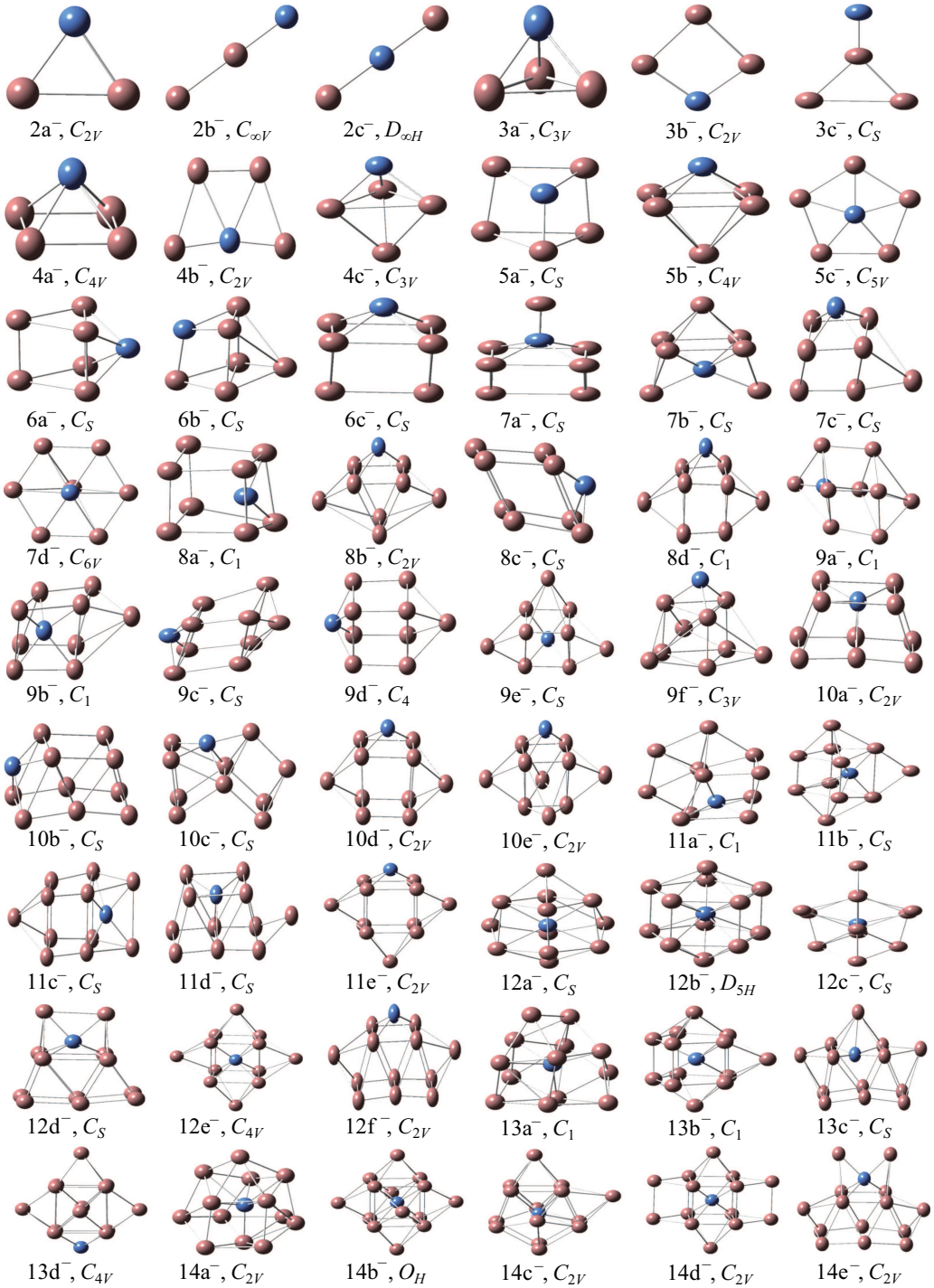


Fig. 2. (color online) The lowest energy and low lying structures of In_nNi^- ($n = 1$–14) clusters.

(ix) In_9Ni, In_9Ni^-, and In_9Ni^+

The ground state structure obtained for In_9Ni has C_1 symmetry and it can be built from In_9Ni (8b) wedge, corresponding to the ^{2}A state. The 3D structure of In_9Ni^- ($9a^-$) with C_1 symmetry is the lowest energy structure, which is different with the most stable neutral In_9Ni. Also, the ground state structure of In_9Ni^+ can be viewed as similar with the neutral In_9Ni.

(x) $In_{10}Ni$, $In_{10}Ni^-$, and $In_{10}Ni^+$

The lowest energy structures of neutral, cationic, and anionic $In_{10}Ni$ clusters adopt the similar C_{2V} structures as shown in the three series (Fig. 1 (10a), 2 ($10a^-$), and 3 ($10a^+$)). Compared with the other neutral clusters of $In_{10}Ni$, the geometric structures of anionic and cationic clusters are quite similar, the symmetries are also same, but the orders of energy change largely, especially for $In_{10}Ni^+$ clusters.

(xi) $In_{11}Ni$, $In_{11}Ni^-$, and $In_{11}Ni^+$

Starting from various initial structures, the $In_{11}Ni$ clusters are calculated considering different spin configurations. The C_1 state (Fig. 1 (11a)) is the lowest energy geometry, corresponding to the electronic state is ^{2}A. The most stable structures of $In_{11}Ni^-$ and $In_{11}Ni^+$ clusters are same with the neutral

$In_{11}Ni$, which the symmetries and the electronic state are C_1 and ^1A, respectively.

(xii) $In_{12}Ni$, $In_{12}Ni^-$, and $In_{12}Ni^+$

When the size of $In_{12}Ni$ cluster is up to 12, the lowest energy of $In_{12}Ni$ with C_S symmetry is obtained by adding one indium atom above the most stable of $In_{11}Ni$. Adding one indium atom in the base of $In_{11}Ni^-$ and $In_{11}Ni^+$ clusters (Fig. 2 ($11a^-$) and Fig. 3 ($11a^+$)), the lowest energy structures for $In_{12}Ni^-$ and $In_{12}Ni^+$ can be also obtained, the structures and the symmetries are consistent with the neutral $In_{12}Ni$.

(xiii) $In_{13}Ni$, $In_{13}Ni^-$, and $In_{13}Ni^+$

The lowest energy structure for neutral $In_{13}Ni$ cluster is similar to its corresponding anionic cluster. This phenomenon is also found for some low-lying isomers (13b and $13b^-$, 13c and $13c^-$, 13d and $13d^-$). Although the lowest energy structure for cationic $In_{13}Ni^+$ is the same as the most stable of $In_{13}Ni$ and $In_{13}Ni^-$, the orders of energy for low-lying $In_{13}Ni^+$ isomers are different with the corresponding the neutral and anionic $In_{13}Ni$ clusters.

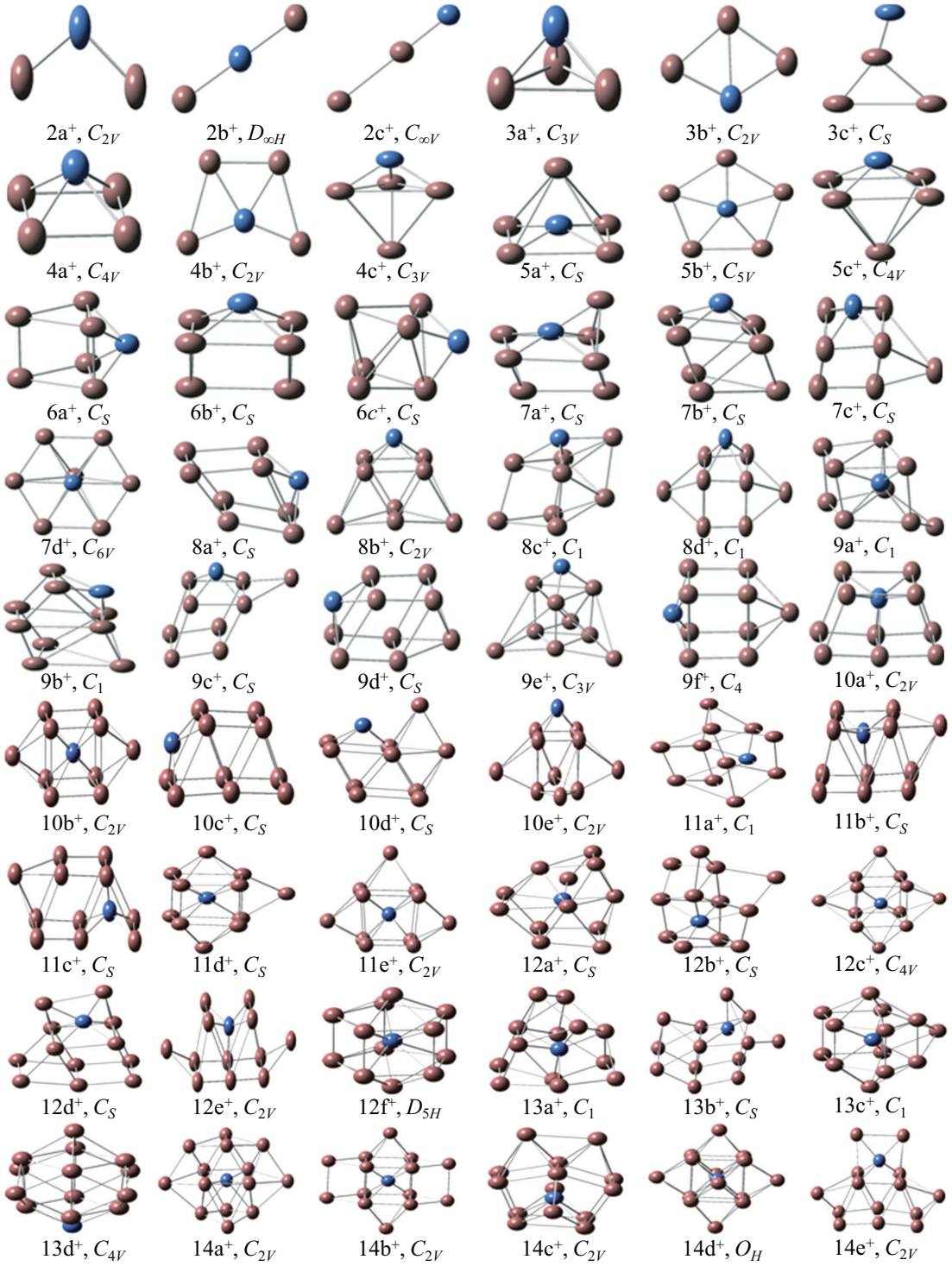


Fig. 3. (color online) The lowest energy and low lying structures of In_nNi^+ ($n = 1$–14) clusters.

(xiv) $In_{14}Ni$, $In_{14}Ni^-$, and $In_{14}Ni^+$

Finally, the ground state structure of $In_{14}Ni$ cluster is obtained by adding one indium on lowest energy of $In_{13}Ni$ cluster (Fig. 1 (14a)), which agrees with the structures of $In_{14}Ni^-$ and $In_{14}Ni^+$ clusters, the symmetries of these clusters are also same, that is C_{2V}. For the other four $In_{14}Ni$ and $In_{14}Ni^-$ clusters, they have the similar structure and the order of energy. Although the structures of $In_{14}Ni^+$ are the same as the $In_{14}Ni$ and $In_{14}Ni^-$ clusters, the order of energy is different.

3.2. Relative stabilities

In order to investigate the strength of chemical bonds, the relative abundances determined in mass spectroscopy experiments, and the thermodynamic stabilities of most stable In_nNi, In_nNi^-, and In_nNi^+ ($n = 1$–14) clusters, we calculated the averaged binding energy (E_b), fragmentation energy (D), and the second-order energy difference ($\Delta_2 E$). The values of the theoretical calculations of In_nNi, In_nNi^-, and In_nNi^+ ($n = 1$–14) clusters are defined in the following formula:

$$E_b[In_nNi] = (nE[In] + E[Ni] - E[In_nNi])/(n+1), \quad (1)$$

$$E_b[In_nNi^-] = ((n-1)E[In] + E[In^-] + E[Ni] - E[In_nNi^-])/(n+1), \quad (2)$$

$$E_b[In_nNi^+] = \left(nE[In] + E[Ni^+] - E[In_nNi^+]\right)/(n+1), \quad (3)$$

$$E_f[In_nNi] = E[In_{n-1}Ni] + E[In] - E[In_nNi], \quad (4)$$

$$E_f[In_nNi^-] = E[In_{n-1}Ni^-] + E[In] - E[In_nNi^-], \quad (5)$$

$$E_f[In_nNi^+] = E[In_{n-1}Ni^+] + E[In] - E[In_nNi^+], \quad (6)$$

$$\Delta_2 E[In_nNi] = E[In_{n+1}Ni] + E[In_{n-1}Ni] - 2E[In_nNi], \quad (7)$$

$$\Delta_2 E[In_nNi^-] = E[In_{n+1}Ni^-] + E[In_{n-1}Ni^-] - 2E[In_nNi^-], \quad (8)$$

$$\Delta_2 E[In_nNi^+] = E[In_{n+1}Ni^+] + E[In_{n-1}Ni^+] - 2E[In_nNi^+], \quad (9)$$

where E is total energy of relevant system. The values of E_b, D, and $\Delta_2 E$ for In_nNi, In_nNi^-, and In_nNi^+ clusters are shown in Figs. 4(a), 4(b), and 4(c), respectively. As seen from Fig. 4(a), the values of averaged binding energy for In_nNi and In_nNi^- clusters show the same growing tendency with cluster size n increasing. The E_b of In_nNi and In_nNi^- clusters increase as the cluster size grows, except $In_5Ni^{(0,-1)}$, $In_8Ni^{(0,-1)}$, and $In_{14}Ni^{(0,-1)}$ clusters, indicating that their neighboring clusters are relatively more stable than $In_5Ni^{(0,-1)}$, $In_8Ni^{(0,-1)}$, and $In_{14}Ni^{(0,-1)}$ clusters. Furthermore, the binding energies of In_nNi^- clusters are larger than the E_b of neutral In_nNi clusters, the results are the same as those reported in Refs. [52]–[54]. However, the curve of In_nNi^+ clusters has a decreasing tendency versus n from 2 to 6, and then, it shows a slight alternation when $n > 6$. A visible peak occurs at $n = 3$, indicating that In_3Ni^+ cluster is relatively more stable than their neighboring clusters. And figure 4(a) clearly illustrates that the binding energy of In_nNi^+ clusters is larger than that of the corresponding In_nNi and In_nNi^- clusters.

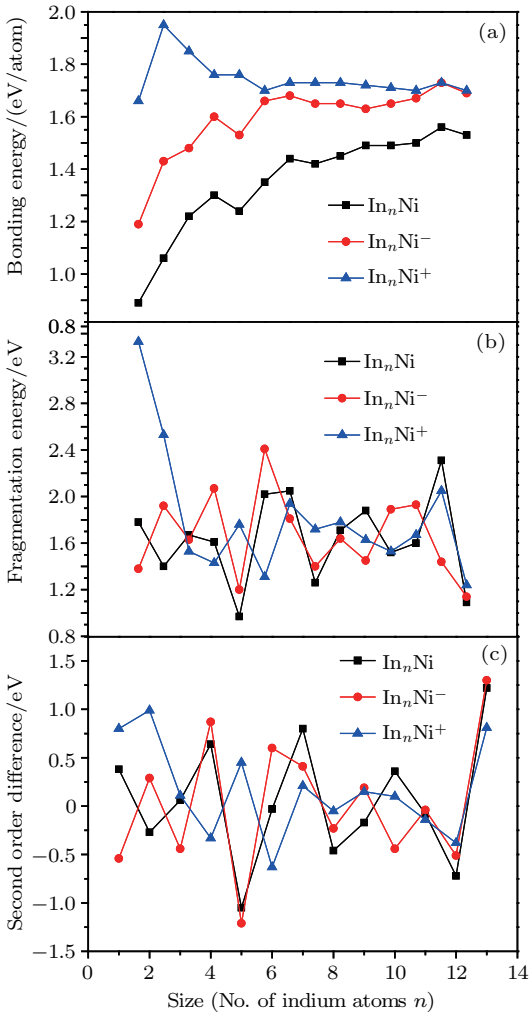


Fig. 4. (color online) Binding energies, fragmentation energies, and the second-order energy difference for the In_nNi, In_nNi^-, and In_nNi^+ ($n = 1$–14) clusters versus the number of indium atoms.

As shown in Fig. 4(b), the D values each exhibit a pronounced odd–even oscillation behavior as a function of cluster size, suggesting that $In_{1,3,7,10,13}Ni$, $In_{2,4,6,9,12}Ni^-$, and $In_{1,5,7,9,13}Ni^+$ clusters keep higher stabilities than their respective corresponding neighbours. For $In_{13}Ni$, In_6Ni^-, and $InNi^+$ clusters, they have the largest fragmentation energy of 2.31 eV, 2.41 eV, and 3.33 eV, respectively. It means that $In_{13}Ni$, In_6Ni^-, and $InNi^+$ clusters are more stable than other clusters. For the second-order energy difference ($\Delta_2 E$) of In_nNi, In_nNi^-, and In_nNi^+ clusters, we observed an odd–even alternation effect in the relative stability as a function of cluster size, that is, maxima are found at $n = 1$, 4, 7, 10, and 13 for neutrals, $n = 2$, 4, 6, 9, 11, and 13 for anions, and $n = 2$, 5, 7, 9, and 13 for cations, respectively, indicating higher stabilities.

3.3. Electronic properties

To obtain the typical electronic properties of In_nNi, In_nNi^-, and In_nNi^+ ($n = 1$–14) clusters, we calculate the

energy gap (E_g) between the highest occupied molecular orbital (HOMO) and the lowest unoccupied molecular orbital (LUMO), the electronic properties including adiabatic electron affinity (AEA), vertical electron detachment energy (VDE), adiabatic ionization potential energy (AIP), vertical ionization potential energy (VIP). The AEA, VDE, AIP, and VIP are calculated as follows:

$$\begin{aligned} \text{AEA} &= E(\text{optimized neutral}) \\ &\quad - E(\text{optimized anion}), \qquad (10) \\ \text{VDE} &= E(\text{neutral at optimized anion geometry}) \\ &\quad - E(\text{optimized anion}), \qquad (11) \\ \text{AIP} &= E(\text{optimized cation}) \\ &\quad - E(\text{optimized neutral}), \qquad (12) \\ \text{VIP} &= E(\text{cation at optimized neutral geometry}) \\ &\quad - E(\text{optimized neutral}), \qquad (13) \end{aligned}$$

where E is the total energies of the corresponding systems.

As presented in Fig. 5(a), for the In_nNi, In_nNi^-, and In_nNi^+ clusters, we find HOMO–LUMO gaps = 1.03 eV–3.48 eV, which indicate that small neutral, cationic and anionic In_nNi clusters are far from a true metal system because the large size of the HOMO–LUMO gaps. The HOMO–LUMO gaps for both the neutral and anion In_nNi clusters have odd–even alteration as the size n increases, except In_3Ni, In_7Ni, In_7Ni^-, In_8Ni^-, and $In_{12}Ni^-$, indicating their relatively higher stabilities, which are in agreement with the second-order energy difference. For the cationic counterpart, there is relatively large gap for cluster $InNi^+$, indicating its large reactive stabilities.

Other important electronic properties that reflect the stability of clusters are their electron affinities and ionization potentials.[50] Comparing the total energies of In_nNi, In_nNi^-, and In_nNi^+ clusters, we obtain the AEA, VDE, AIP, and VIP. Figure 5(b) depicts the variations of AEA and VDE of In_nNi clusters with the number of indium atoms. The AEA values tend to increase as n increases, except In_7Ni, In_9Ni, and $In_{10}Ni$. When $n = 2$, 6, 8, and 14, the AEA values are higher than those of adjacent clusters, reflecting the higher stability of In_2Ni^-, In_6Ni^-, In_8Ni^-, and $In_{14}Ni^-$. As for VDE, the calculated maximums at $n = 1$, 5, 8, 12, and 14, the minima at $n = 2$, 6, 10, and 13. As shown in Fig. 5(c), the VIP gives the lower bound while the AIP gives the upper bound. The difference of the variation trend of AIP and VIP for the same cluster size is small, because the geometries of these cationic clusters do not differ greatly from the corresponding neural clusters. On the other hand, the difference between AIP and VIP for the same cluster size is great, since the geometries of these cations differ significantly from the corresponding neutral clusters. The AIP values of In_5Ni and In_9Ni are smaller, indicating that these clusters are more easily ionized than the others.

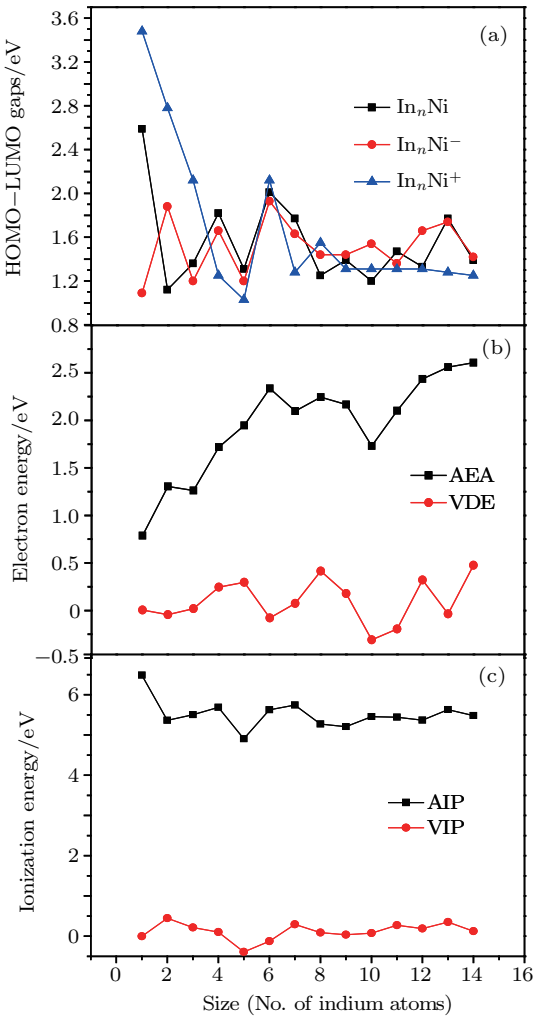


Fig. 5. (color online) HOMO–LUMO gaps, electron energies, and ionization energies for the In_nNi, In_nNi^-, and In_nNi^+ (n = 1–14) clusters versus the number of indium atoms.

3.4. Magnetisms

The total magnetic moments of the studied $In_nNi^{(0,\pm1)}$ (n = 1–14) clusters are plotted as a function of cluster sizes in Fig. 6. From Fig. 6, we see that the total magnetic moments of the In_nNi clusters show an obvious odd–even alternative behavior, expect In_9Ni. When n is odd, the total magnetic moments decrease with cluster size n increases, this phenomenon is also happened when n is even. We also observed that the total magnetic moments of the $In_nNi^{\pm1}$ clusters show an obvious odd–even alternative behavior, expect for $In_{10,11,12}Ni^-$, In_2Ni^+. The $In_nNi^{\pm1}$ clusters exhibit nonmagnetic moments for odd n, expect for $InNi^{\pm1}$, In_9Ni^-. That is because these clusters are a closed-shell system, whose α and β spin orbitals degenerate, so the corresponding magnetic moment is zero. Whereas for even n, the magnetic moments of $In_nNi^{\pm1}$ clusters decrease with cluster size n increases, in which the magnetism may come from the even number of valence electrons.

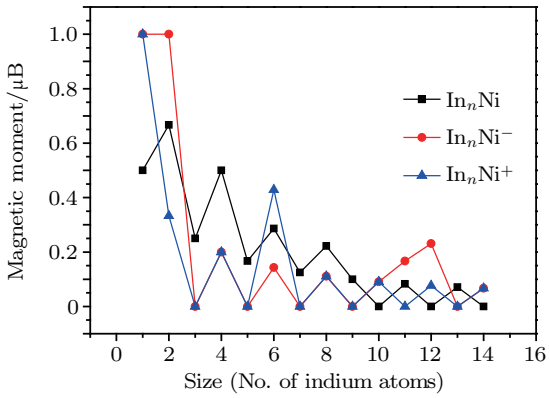


Fig. 6. (color online) Magnetic moment for the In_nNi, In_nNi^-, and In_nNi^+ ($n = 1$–14) clusters versus the number of indium atoms.

3.5. Natural population analysis

The localization of charge and the charge-transfer information of $In_nNi^{(0,\pm1)}$ ($n = 1$–14) clusters will be provided by the natural population analysis (NPA), the results are displayed in Table 2. In neutral In_nNi clusters, the charge on In atom in the ground state isomers has positive values and Ni has negative values. This phenomenon indicates that the electrons in In_nNi clusters are transferred from In frames to Ni atom. Thus, the In frames act as electron donor in In_nNi clusters. Less than an electron is transferred from In frames to Ni atom, which shows that the bonds between indium and nickel atoms are covalent rather than ionic. The charges on all the In and Ni atoms of anionic In_nNi clusters have negative values, which may be related to the arrangement of the internal charge induced by the extra electron. For In_nNi^+ clusters, as shown in Table 2, the indium atoms possess positive charges in the range of 0.654–1.444 electrons, while the nickel atoms possess negative charges, except $InNi^+$ and In_6Ni^+. It indicates that the charges are transferred from In frames to Ni atom, which is identical to the situation in neutral clusters.

Table 2. The total charges (Q) of In atoms and the charges (Q) of Ni atom for the ground state structures of $In_nNi^{(0,\pm1)}$ clusters.

	Q (In)	Q (Ni)		Q (In)	Q (Ni)		Q (In)	Q (Ni)
InNi	0.263	–0.263	$InNi^-$	–0.423	–0.577	$InNi^+$	0.654	0.356
In_2Ni	0.462	–0.462	In_2Ni^-	–0.319	–0.681	In_2Ni^+	1.228	–0.228
In_3Ni	0.216	–0.216	In_3Ni^-	–0.747	–0.253	In_3Ni^+	1.279	–0.279
In_4Ni	0.142	–0.142	In_4Ni^-	–0.937	–0.063	In_4Ni^+	1.127	–0.127
In_5Ni	0.069	–0.069	In_5Ni^-	–0.892	–0.108	In_5Ni^+	1.314	–0.314
In_6Ni	0.013	–0.013	In_6Ni^-	–0.872	–0.128	In_6Ni^+	0.897	0.103
In_7Ni	0.173	–0.173	In_7Ni^-	–0.853	–0.147	In_7Ni^+	1.105	–0.105
In_8Ni	0.038	–0.038	In_8Ni^-	–0.834	–0.166	In_8Ni^+	1.024	–0.024
In_9Ni	0.141	–0.141	In_9Ni^-	–0.840	–0.160	In_9Ni^+	1.025	–0.025
$In_{10}Ni$	0.223	–0.223	$In_{10}Ni^-$	–0.860	–0.140	$In_{10}Ni^+$	1.066	–0.066
$In_{11}Ni$	0.103	–0.103	$In_{11}Ni^-$	–0.902	–0.098	$In_{11}Ni^+$	1.032	–0.032
$In_{12}Ni$	0.351	–0.351	$In_{12}Ni^-$	–0.665	–0.335	$In_{12}Ni^+$	1.249	–0.249
$In_{13}Ni$	0.519	–0.519	$In_{13}Ni^-$	–0.450	–0.550	$In_{13}Ni^+$	1.412	–0.412
$In_{14}Ni$	0.507	–0.507	$In_{14}Ni^-$	–0.552	–0.448	$In_{14}Ni^+$	1.444	–0.444

4. Conclusions

In this work, we performed a systematic study of the neutral, anionic, and cationic In_nNi clusters. We obtained the most stable structures for $In_nNi^{(0,\pm1)}$ clusters, the optimized results indicate that the In_nNi and the In_nNi^+ clusters keep the similar structures, the lowest energy structures of In_nNi^- clusters also maintain the analogous structures as $In_nNi^{(0,+1)}$ clusters, except In_8Ni^- and In_9Ni^-. On the basis of the structures and energies from our systematic calculations, we analyzed the relative stabilities by calculating the averaged binding energy, the fragmentation energy, and the second-order energy difference. We show that the binding energy of In_nNi^+ clusters is larger than that of the corresponding In_nNi and In_nNi^- clusters, the fragmentation energy and the second-order energy difference exhibit a pronounced odd–even oscillation behavior as a function of the cluster size. On the basis of the calculated HOMO–LUMO gaps, AEA, VDE, AIP, and VIP, it is found that the neutral, anionic, and cationic In_nNi clusters are far from a true metal system due to the large size of the HOMO–LUMO gaps, In_5Ni and In_9Ni clusters are more easily ionized than the others because they have smaller AIP. We also observed that the total magnetic moments of the $In_nNi^{\pm1}$ clusters show an obvious odd–even alternative behavior. The natural population analysis results of $In_nNi^{(0,+1)}$ clusters indicate that the charges transfer from In frames to the Ni atom.

References

[1] Santos C L dos, Schhmidt T M and Piquini P 2011 *Nanotechnology* **22** 265203
[2] Rayane D, Melinon P, Cabaud B, Hoareau A, Tribollet B and Broyer M 1989 *J. Chem. Phys.* **90** 3295
[3] Ma Z, Coon S R, Calaway W F, Gruen M J and Von NagyFelsobuki E L 1994 *J. Vac. Sci. Technol. A* **12** 2425
[4] Baguenard B, Pellain M, Bordas C, Lermé J, Vialle J L and Broyer M 1993 *Chem. Phys. Lett.* **205** 13
[5] Staudt C, Wucher A, Neukermans S, Janssens E, Vanhoutte F, Vandeweert E, Silverans R E and Lievens P 2002 *Nucl. Instrum. Method Phys. Res. B* **193** 787
[6] Lermé J, Dugourd P, Hudgins R R and Jarrold M F 1999 *Chem. Phys. Lett.* **304** 19

[7] Zhang W Q, Zhao G F, Sun J M, Zhi L L and Gu Y Z 2009 *Chem. Phys.* **361** 44
[8] Froben F W, Schulze W and Kloss U 1983 *Chem. Phys. Lett.* **99** 500
[9] Onwuagba B N 1993 *Phys. Stat. Sol.* **180** 391
[10] King R B, Silaghi-Dumitrescu I and Kun A 2001 *Inorg. Chem.* **40** 2450
[11] Staudt C and Wucher A 2002 *Phys. Rev. B* **66** 075419
[12] Janssens E, Neukernans S, Vanhoutte F, Silverans R E, Lievens P, Navarro-Vázquez A and Schleyer P V R 2003 *J. Chem. Phys.* **118** 5862
[13] Zhang W Q, Sun J M, Zhao G F and Zhi L L 2008 *J. Chem. Phys.* **129** 064310
[14] Longo R C, Carrete J, Aguilera-Granja F, Vega A and Gallego L J 2009 *J. Chem. Phys.* **131** 074504
[15] Ding J N Yuan N Y, Li C L, Wang X Q, Chen G G, Chen X S and Lu W 2011 *J. Appl. Phys.* **109** 014322
[16] Zhang W Q, Liu T G and Bai Y Z 2012 *Comput. Theor. Chem.* **986** 57
[17] Liu Y Z, Deng K M, Yuan Y B, Chen X, Wu H P and Wang X 2009 *Chem. Phys. Lett.* **469** 321
[18] Chroneos A, Kube R, Bracht H, Grimes R W and Schwingenschlögl U 2010 *Chem. Phys. Lett.* **490** 38
[19] Melko J J, Ong S V, Gupta U, Reveles J U, D'Emidio J, Khanna S N and Castleman A W Jr 2010 *Chem. Phys. Lett.* **500** 196
[20] Liu Y Z, Yuan Y B, Xiao C Y and Deng K M 2013 *Chem. Phys. Lett.* **583** 131
[21] Demaria G, Drowart J and Inghram M G 1959 *J. Chem. Phys.* **31** 1076
[22] Li Z J and Li J H 2008 *Chin. Phys. B* **17** 2951
[23] Nakajima A, Hoshino K, Sugioka T, Naganuma T, Taguwa T, Yamada Y, Watanabe K and Kaya K 1993 *J. Phys. Chem.* **97** 86
[24] Costales A, Kandalam A and Pandey R 2003 *J. Phys. Chem. B* **107** 4508
[25] Roy S and Springborg M 2003 *J. Phys. Chem. B* **107** 2771
[26] Bernstein J, Armon E, Zemel E and Kolodney E 2013 *J. Phys. Chem. A* **117** 11856
[27] Gupta U, Reveles J U, Melko J J, Khanna S N and Castleman A W Jr 2010 *J. Phys. Chem. C* **114** 15963
[28] Melko J J, Ong S V, Gupta U, Reveles J U, D'Emidio J, Khanna S N and Castleman A W Jr 2010 *J. Phys. Chem. C* **114** 20907
[29] Costales A, Kandalam A K, Pendás A M, Blanco M A, Recio J M and Pandey R 2000 *J. Phys. Chem. B* **104** 4368
[30] Heinebrodt M, Malinowski N, Tast F, Branz W, Billas I M L and Martin T P 1999 *J. Chem. Phys.* **110** 9915
[31] Costatles A and Pandey R 2002 *Chem. Phys. Lett.* **362** 210
[32] Shi S P, Liu Y L, Deng B L, Zhang C Y and Jiang G 2014 *Comput. Mater. Sci.* **95** 476
[33] Shi S P, Cao Y P, Zhai A P, Li Y and Jin X X 2011 *Physica B* **406** 3544
[34] Wang J and Han J G 2006 *J. Phys. Chem. B* **110** 7820
[35] Bandyopadhyay D and Sen P 2010 *J. Phys. Chem. A* **114** 1835
[36] Yuan D W, Wang Y and Zeng Z 2005 *J. Chem. Phys.* **122** 114310
[37] Ren Z Y, Li F, Guo P and Han J G 2005 *Mol. J. Struc.: Theor.* **718** 165
[38] Bailey M S, Wilson N T, Roberts C and Johnston R L 2003 *Eur. Phys. J. D* **25** 41
[39] Neukermans S, Janssens E, Tanaka H, Silverans R E and Lievens P 2003 *Phys. Rev. Lett.* **90** 033401
[40] Guo L J, Zhao G F, Gu Y Z, Liu X and Zeng Z 2008 *Phys. Rev. B* **77** 195417
[41] Becke A D 1988 *Phys. Rev. A* **38** 3098
[42] Lee C, Yang W and Parr R G 1988 *Phys. Rev. B* **37** 785
[43] Bergner A, Dolg M, KÜchle W, Stoll H and Preuß H 1993 *Mol. Phys.* **80** 1431
[44] Frisch M J, Trucks G W, Schlegel H B, Scuseria G E, Robb M A, Cheeseman J R, Montgomery J A Jr, Vreven T, Kudin K N, Burant J C, Millam J M, Iyengar S S, Tomasi J, Barone V, Mennucci B, Cossi M, Scalmani G, Rega N, Petersson G A, Nakatsuji H, Hada M, Ehara M, Toyota K, Fukuda R, Hasegawa J, Ishida M, Nakajima T, Honda Y, Kitao O, Nakai H, Klene M, Li X, Knox J E, Hratchian H P, Cross J B, Adamo C, Jaramillo J, Gomperts R, Stratmann R E, Yazyev O, Austin A J, Cammi R, Pomelli C, Ochterski J W, Ayala P Y, Morokuma K, Voth G A, Salvador P, Dannenberg J J, Zakrzewski V G, Dapprich S, Daniels A D, Strain M C, Farkas O, Malick D K, Rabuck A D, Raghavachari K, Foresman J B, Ortiz J V, Cui Q, Baboul A G, Clifford S, Cioslowski J, Stefanov B B, Liu G, Liashenko A, Piskorz P, Komaromi I, Martin R L, Fox D J, Keith T, Al-Laham M A, Peng C Y, Nanayakkara A, Challacombe M, Gill P M W, Johnson B, Chen W, Wong M W, Gonzalez C and Pople J A 2003 Gaussian 03, Revision B 02, Gaussian, Inc, Pittsburgh PA
[45] Downs A J 1933 *Chemistry of Aluminium, Gallium, Indium, and Thallium* (London: Blackie Academic & Professional)
[46] Drowart J and Honig R E 1957 *J. Phys. Chem.* **61** 980
[47] Gutsev G L and Bauschlicher Jr C W 2003 *J. Phys. Chem. A* **107** 4755
[48] Morse M D, Hansen G P, Langridge-Smith P R R, Zheng L S, Geusic M E, Michalopoulos D L and Smalley R E 1984 *J. Chem. Phys.* **80** 5400
[49] Wang H M, Haouari H, Craig R, Lombardi J R and Lindsay D M 1996 *J. Chem. Phys.* **104** 3420
[50] Xing X D, Hermann A, Kuang X Y, Ju M, Lu C, Jin Y Y, Xia X X and Maroulis G 2016 *Sci. Rep.* **6** 19656
[51] Shi S P, Liu Y L, Li Y. Deng B L, Zhang C Y and Jang G 2016 *Comput. Theor. Chem.* **1079** 47
[52] Xing X D, Wang J J, Kuang X Y, Xia X X, Lu C and Maroulis G 2016 *Phys. Chem. Chem. Phys.* **18** 26177
[53] Sun W G, Wang J J, Lu C, Xia X X, Kuang X Y and Hermann A 2017 *Inorg. Chem.* **56** 1241
[54] Xia X X, Kuang X Y, Lu C, Jin Y Y, Xing X D, Merino G and Hermann A 2016 *J. Phys. Chem. A* **120** 7947